

07.3

Experimental implementation of reservoir computing with a semiconductor laser subject to optoelectronic feedback

© G.O. Danilenko, D.A. Pavlov, E.A. Viktorov, A.V. Kovalev

ITMO University, St. Petersburg, Russia
E-mail: avkovalev@itmo.ru

Received April 23, 2024

Revised May 8, 2024

Accepted May 13, 2024

We present the results of experimental research of a reservoir computing system based on a semiconductor laser with optoelectronic feedback. In the research, the memory capacity of the system and error in predicting the chaotic Mackey–Glass time series have been determined. The effect of the system pump current, feedback strength and number of nodes on its performance has been investigated.

Keywords: reservoir computing, semiconductor lasers, optoelectronic feedback.

DOI: 10.61011/TPL.2024.09.59147.19971

Reservoir computing (RC) is a machine learning approach, which is based on dynamic system's nonlinear response to an input signal. The RC systems are used for solving time-dependent problems and analyzing big data. Their distinctive features are a simplified approach to the system training and energy efficiency, stemming from their implementation based on physical devices. There have already been experimentally demonstrated systems based on optoelectronic oscillators [1,2], semiconductor lasers with optical feedback (FB) [3], and photonic integrated circuits [4]. Among physical, and, in particular, optical implementations of the RC, time-delay systems [5] are especially widespread. The time-delay RC (TDRC) systems are based on using a single nonlinear node and time-delayed FB. Along with this, time multiplexing is used to create N virtual nodes similar to those of recurrent neural networks, which are distributed in the FB loop at fixed time intervals t_N [3,5].

In this work, the TDRC system based on an optoelectronic-FB semiconductor laser, which was previously considered in theoretical works [6–8], has been studied experimentally. Dependencies of its memory capacity and error in predicting the chaotic time series on the system parameters have been determined.

Schematic diagram of the experimental setup is given in Fig. 1. This setup employs standard optical components with single-mode fiber leads with FC/APC connectors. It is insensitive to changes in the optical field polarization state and phase. A single-frequency continuously-emitting laser source is used to implement this approach. The modulation bandwidth of the laser pump current determines the frequency of data input to the system and the number of virtual nodes, which is achievable in the system in question (see below). In this work, we used a distributed-feedback laser diode Nolatech DFB-1550-14BF (LD) with the wavelength of 1550 nm, threshold current of 9 mA, and output power of 5 mW at the current of 40 mA, which

temperature was stabilized by using a temperature controller ELECDEMO KW_DFB (TC). The LD was powered by a stabilized current source Keysight N6705C (CS). The laser radiation passed through the optical isolator (OI) and was converted to the electrical signal by photodetector Alphas UPD-15-IR2-FC (PD); a part of the photodetector output signal was recorded by an oscilloscope Keysight UXR0204A and used to register the values of the RC system nodes; another signal part was fed into the FB loop. The FB electronic part consisted of a non-inverting radio-frequency (RF) signal amplifier WYDZ-LNA-10M-6GHz 30 dB (RFA1), an attenuator DYKB DC-6GHz with the attenuation coefficient varying with the 0.25 dB step (ATT), an RF signal combiner SHWLCB2-204000S (COMB), an inverting amplifier Mini-Circuits ZX60-V82-S+ 20-6000MHz 13 dB (RFA2), a signal inverter (INV), and a bias tee Mini-Circuits ZX85-12G-S+ (BT). The input signal was fed into the system by means of an arbitrary-waveform generator Keysight M8195A.

The system FB strength k_{fb} is defined as the total gain: $k_{fb} = k_1 - k_a + k_2$, where $k_{1,2}$ is the fixed gain of

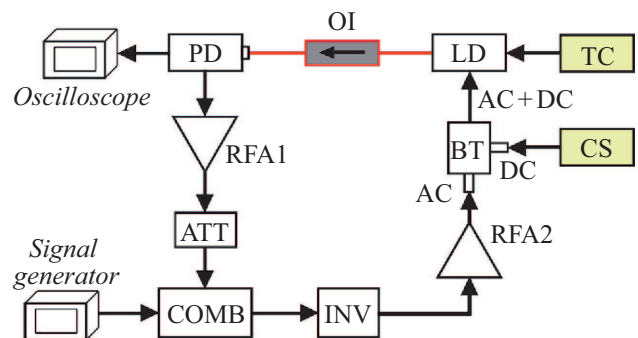


Figure 1. Schematic diagram of the optoelectronic reservoir computing system. Red lines represent the optical signal; black lines are for the electrical signal. The figure variant with colored lines is given in the paper electronic version.

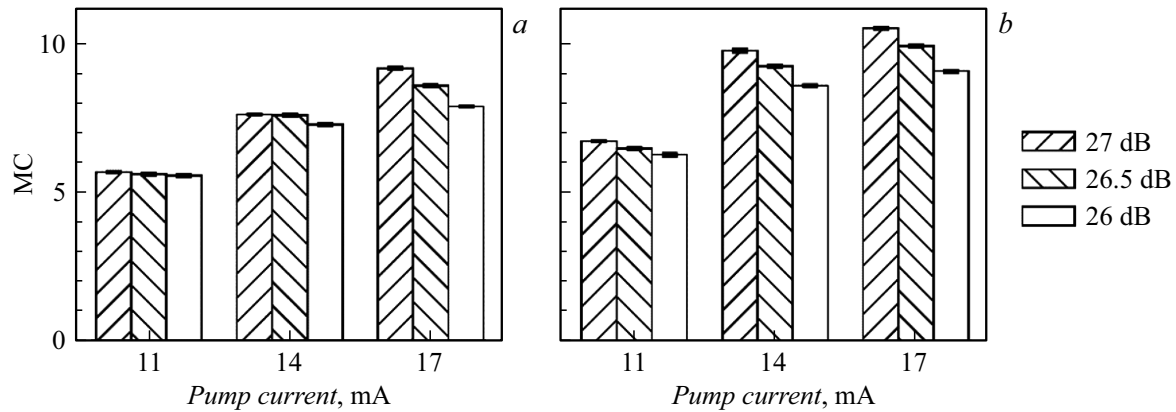


Figure 2. The system memory capacity (MC) versus the pump current and feedback strength. $N = 20$ (a) and 40 (b).

RFA1 (RFA2) equal to 30 (13) dB, k_a is the variable attenuation coefficient of the attenuator that is used to change the feedback strength. The FB signal delay time, determined experimentally by using rectangular pulses from the waveform generator, is 23.8 ns, which corresponds to the round-trip frequency of 42 MHz. The RC system energy consumption is no more than 2 W (besides the energy consumption of the generator and the oscilloscope).

Input signals are entered into the RC system sequentially by modulating the LD pump current. A single value input time $T_S = Nt_N$ is made close to the FB signal delay time but slightly different so to eliminate resonance effects that significantly degrade the system performance [8]. To set the weights of the reservoir input layer, each input value S_i at the i -th input step is modulated during the input time by a so-called mask [5], that is, a piecewise constant function with random fixed values different at each interval t_N , which is defined for time interval T_S . The RC output value is calculated by multiplying the LD intensity, recorded by PD and oscilloscope at time moments related to the virtual nodes, and the output layer weight coefficients, determined at the training stage via linear regression [5,9].

The best performance of the system was previously predicted theoretically to be near the instability boundary of the stationary lasing state [6,7], which was found experimentally at $k_{fb} = 27$ dB ($k_a = 16$ dB) for the pump current of 9–25 mA. The bandwidth of the laser pump current modulation at the -10 dB level is limited to the frequency of 1.4 GHz, while the FB passband is 0.01–2 GHz. The RC system performance was studied depending on the FB strength, the LD pump current and the number of the system nodes N . The symbol input frequency $1/T_S = 40$ MHz determines the pump current modulation frequency and, hence, the laser power modulation frequency as $1/t_N = 1/(T_S N) = 0.8$ and 1.6 GHz for 20 and 40 nodes, respectively. To ensure synchronous reading of virtual nodes, the PD output signals were recorded with an oscilloscope with the sampling frequency multiple to the pump current modulation frequency: 4 and 8 GHz for 20 and 40 nodes, respectively. To find standard deviation for

each measured characteristic of the system, the RC process was repeated five times.

The memory capacity (MC) characterizes the system's ability to restore the previously entered data [9]. It is defined as

$$MC = \sum_{d=1}^{\infty} mc_d = \sum_{d=1}^{\infty} \frac{\text{cov}^2(O_i, S_{i-d})}{\sigma^2(O_i)\sigma^2(S_i)}, \quad (1)$$

where mc_d is the memory function, cov is the covariance, O_i is the output value at the i -th input step, S_{i-d} is the input value entered d steps earlier, σ^2 is the dispersion. Memory function mc_d represents the relationship of the reservoir output data with input data entered d steps earlier [10]. The input signal was generated by a sequence of 5000 random values uniformly distributed in the $[-1,1]$ interval. Fig. 2 presents experimental MC values versus the pump current and feedback strength. The largest memory capacity is 10.5 for $N = 40$, $k_{fb} = 27$ dB and pump current of 17 mA. The increase in pump current leads to an increase in memory capacity, i.e. the system becomes more linear. In [3] where a physical laser-based RC system was also implemented, the memory capacity did not exceed 8. In our RC system, the memory capacity increases only slightly with the node number increase to $N = 40$, which may be due to the fact that the LD modulation bandwidth and FB passband are limited.

By solving the task of predicting a chaotic time series of the Mackey–Glass system, it is possible to evaluate the RC systems ability to predict the series values one step ahead [3]. The dynamic Mackey–Glass system is defined as

$$\frac{dy(t)}{dt} = \frac{\alpha y(t-\tau)}{1+y^\beta(t-\tau)} - \gamma y(t), \quad (2)$$

where $\alpha = 0.2$, $\beta = 10$, $\gamma = 0.1$ and $\tau = 17$. To obtain the time series, equation (2) was solved by the Euler method with the step of 0.17 with every third point being kept [3].

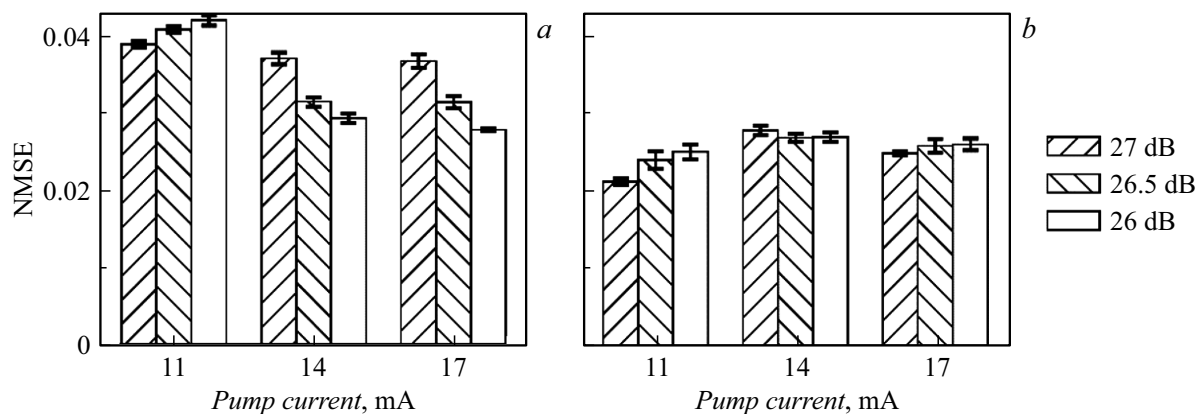


Figure 3. Error (NMSE) in predicting the time series of the Mackey–Glass chaotic system versus the pump current and feedback strength. $N = 20$ (a) and 40 (b).

The prediction error is estimated as the normalized root mean square error (NMSE):

$$\text{NMSE} = \frac{1}{L} \sum_{i=1}^L \frac{(Y_i - O_i)^2}{\sigma^2(Y_i)}, \quad (3)$$

where L is the test sample length equal to 1500, Y_i is the target value at the time series i -th step defined by (2), O_i is the i -th step value predicted by the system. In this problem, the prediction error varied in the range of 0.02–0.04 (Fig. 3), which is comparable with the results of [1,3], while relative standard deviation did not exceed 4%, which confirms stable repeatability of calculations.

Thus, in this work we have studied experimentally a semiconductor-laser-based reservoir computing system with optoelectronic feedback, which is characterized by low power consumption (no more than 2 W). We have determined the system's memory capacity which maximum value is ~ 10 and solved the problem of predicting the Mackey–Glass system time series with the lowest prediction error of 0.02. The results point to perspectives of the system under consideration.

Funding

The study was supported by the Russian Science Foundation (project № 23-72-01050 (<https://rscf.ru/project/23-72-01050/>)).

Conflict of interests

The authors declare that they have no conflict of interests.

References

[1] M.C. Soriano, P. Massuti-Ballester, J. Yelo, I. Fischer, in *ICANN 2019: Workshop and special sessions*, ed. by I. Tetko, V. Kůrková, P. Karpov, F. Theis. Lecture Notes in Computer Science (Springer, Cham, 2019), vol. 11731. p. 170–174. DOI: 10.1007/978-3-030-30493-5_18

- [2] Y. Chen, L. Yi, J. Ke, Z. Yang, Y. Yang, L. Huang, Q. Zhuge, W. Hu, *Opt. Express*, **27** (20), 27431 (2019). DOI: 10.1364/OE.27.027431
- [3] J. Bueno, D. Brunner, M.C. Soriano, I. Fischer, *Opt. Express*, **25** (3), 2401 (2017). DOI: 10.1364/OE.25.002401
- [4] K. Harkhoe, G. Verschaffelt, A. Katumba, P. Bienstman, G. Van der Sande, *Opt. Express*, **28** (3), 3086 (2020). DOI: 10.1364/OE.382556
- [5] L. Appeltant, M.C. Soriano, G. Van der Sande, J. Danckaert, S. Massar, J. Dambre, B. Schrauwen, C.R. Mirasso, I. Fischer, *Nat. Commun.*, **2**, 468 (2011). DOI: 10.1038/ncomms1476
- [6] P.S. Dmitriev, A.V. Kovalev, A. Locquet, D. Rontani, E.A. Viktorov, *Opt. Lett.*, **45** (22), 6150 (2020). DOI: 10.1364/OL.405177
- [7] G.O. Danilenko, A.V. Kovalev, E.A. Viktorov, A. Locquet, D.S. Citrin, D. Rontani, *Chaos*, **33** (1), 013116 (2023). DOI: 10.1063/5.0127661
- [8] G.O. Danilenko, A.V. Kovalev, E.A. Viktorov, A. Locquet, D.S. Citrin, D. Rontani, *Chaos*, **33** (1), 113125 (2023). DOI: 10.1063/5.0172039
- [9] L. Larger, A. Baylón-Fuentes, R. Martinenghi, V.S. Udaltsov, Y.K. Chembo, M. Jacquot, *Phys. Rev. X*, **7** (1), 011015 (2017). DOI: 10.1103/PhysRevX.7.011015
- [10] H. Jaeger, *Short term memory in echo state networks*, GMD report (GMD Forschungszentrum Informationstechnik, St. Augustin, 2002), vol. 152. DOI: 10.24406/publica-fhg-291107

Translated by EgoTranslating